A conserved flavin-shielding residue regulates NO synthase electron transfer and nicotinamide coenzyme specificity

Subrata Adak*, Manisha Sharma, Abigail L. Meade, and Dennis J. Stuehr*

Department of Immunology, Lerner Research Institute, Cleveland Clinic, Cleveland, OH 44195

Edited by Louis J. Ignarro, University of California School of Medicine, Los Angeles, CA, and approved August 1, 2002 (received for review May 10, 2002)

Nitric oxide synthases (NOSs) are flavoheme enzymes that contain a ferredoxin:$NADP^+$-reductase (FNR) module for binding NADPH and FAD and are unusual because their electron transfer reactions are controlled by the Ca^{2+}-binding protein calmodulin. A conserved aromatic residue in the FNR module of NOS shields the isoalloxazine ring of FAD and is known to regulate NADPH binding affinity and specificity in related flavoproteins. We mutated Phe-1395 (F1395) in neuronal NOS to Tyr and Ser and tested their effects on nucleotide coenzyme specificity, catalytic activities, and electron transfer in the absence or presence of calmodulin. We found that the aromatic side chain of F1395 controls binding specificity with respect to NADH but does not greatly affect affinity for NADPH. Measures of flavin and heme reduction kinetics, ferricyanide and cytochrome *c* reduction, and NO synthesis established that the aromatic side chain of F1395 is required to repress electron transfer into and out of the flavins of neuronal NOS in the calmodulin-free state, and is also required for calmodulin to fully relieve this repression. We speculate that the phenyl side chain of F1395 is part of a conformational trigger mechanism that negatively or positively controls NOS electron transfer depending on the presence of calmodulin. Such use of the conserved aromatic residue broadens our understanding of flavoprotein structure and regulation.

Nitric oxide (NO) is generated by NO synthases (NOSs) and modulates physiology and pathology in mammals (1, 2). The NOS polypeptide consists of an N-terminal oxygenase domain that contains heme, 6*R*-tetrahydrobiopterin (H_4B), and an L-arginine (Arg) binding site, and a C-terminal reductase domain that contains FMN, FAD, and an NADPH binding site (3–5). An ≈20-aa calmodulin (CaM) binding site is located between the reductase and oxygenase domains (3–5). During NO synthesis, electrons from NADPH transfer in a linear sequence to FAD, FMN, and then to the heme, which binds and activates dioxygen (3–5). Although NOS oxygenase domains have unusual structure (6–8), NOS reductase domains are structurally similar to other NADPH-requiring flavoproteins like cytochrome P450 reductase (CYPR), sulfite reductase flavoprotein, methionine synthase reductase, and cytochrome P450BM3 (9–11). These flavoproteins are all comprised of a flavodoxin module that contains FMN and a ferredoxin:$NADP^+$ reductase (FNR) module that contains FAD and the NADPH binding site (12).

NOS catalysis is controlled by varied mechanisms (3–5, 13). Surprisingly, its electron transfer events are regulated by Ca^{2+}-dependent CaM binding (14). Although this is unusual for a redox enzyme, it may be representative of a growing class of Ca^{2+}-activated flavoproteins that include NADPH oxidases (15) and a flavoprotein of *Desulfovibrio gigas* (16). In NOS, CaM binding relieves a kinetic repression on electron transfer both into and out of its reductase domain (17, 18). We are only beginning to understand the basis for the repression or how it is relieved by CaM. Recent studies implicate two control elements that are unique to the NOS reductase domain. One element is represented by a 42-aa "insert" in the neuronal NOS (nNOS) FMN module, whereas the other is represented by a 33-aa C-terminal extension at the C terminus (19–22). Deletion of either control element showed that each has a role in modulating Ca^{2+} sensitivity, repression of electron transfer, and its relief on CaM binding (19–26). Although this work has established the importance of either control element, it is still unclear as to how they transmit their effects into the core flavoprotein structure of NOS.

We addressed this issue through point mutagenesis of Phe-1395 (F1395) that lies penultimate to the start of the C-terminal control element in rat nNOS. A recent crystal structure of an FNR fragment of nNOS confirmed that F1395 is representative of conserved aromatic residues that are located near the C terminus of related FNR-like flavoproteins (12, 27). In these flavoproteins, the side chain of the conserved aromatic residue shields FAD through a π-stacking interaction with its isoalloxazine ring (Fig. 1). The aromatic residue thus plays an important role in adjusting the nucleotide accessibility for hydride transfer between NADPH and FAD. To allow the required stacking interaction between reduced nicotinamide and FAD, the aromatic side chain needs to flip away (12, 27) as indicated in various crystal structures of $NADP^+$-bound FNR, CYPR, or glutathione reductase (27–29). Indeed, studies with FNR and CYPR mutants showed that the aromatic side chain modulates their NADPH-binding affinity and selectivity, but does not modulate their electron transfer reactions (30–31). In contrast, our current work reveals that the aromatic side chain of F1395 has a decreased importance in modulating nNOS nucleotide affinity and selectivity, and instead plays a key role in transducing the effects of CaM and the C-terminal control element on nNOS electron transfer and associated catalysis. Thus, nNOS demonstrates a previously undocumented use for this conserved structural motif regarding control of electron transfer.

Materials and Methods

Materials. All regents and materials were obtained from Sigma or reported sources (32–34).

Molecular Biology. Restriction digestions, cloning, bacterial growth, transformation, and isolation of DNA fragments were performed by using standard procedures. Rat nNOS DNA was inserted into the 5′ *Nde*I and 3′ *Xba*I site into the pCWori vector (32–34). The F1395Y and F1395S mutation site in the nNOS cDNA was constructed by subcloning a PCR-generated fragment from pCWori/nNOS with a 5′ oligonucleotide containing a newly engineered mutational site. The nNOS cDNA fragment coding from the *Kpn*I unique restriction site at position 4514 to the *Xba*I restriction site at position 4785 was amplified by using

This paper was submitted directly (Track II) to the PNAS office.

Abbreviations: NOS, NO synthase; nNOS, neuronal NOS; EPPS, 4-(2-hydroxyethyl)-1-piperazinepropanesulfonic acid; CaM, calmodulin; CYPR, cytochrome P-450 reductase; FNR, ferredoxin:$NADP^+$ reductase.

*To whom correspondence may be addressed at: Immunology NB-3, Lerner Research Institute, Cleveland Clinic, 9500 Euclid Avenue, Cleveland, OH 44195. E-mail: stuehrd@ccf.org or adaks@ccf.org.

www.pnas.org/cgi/doi/10.1073/pnas.192283399

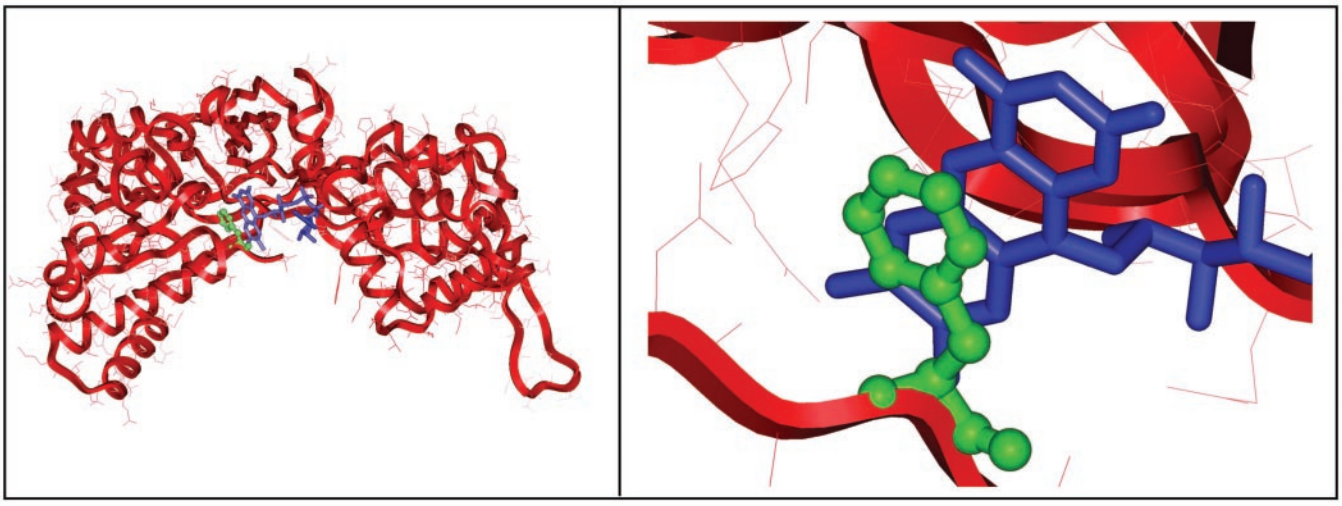

```
E. coli SIR-FP      593RYQRDVY
C.elegans MSR       675QYIEDVWG
Spinach FNR         363QWNVEVY
Rat CYPR            671RYSLDVWS
Mouse iNOS         1116RYHEDIFGAVFSYGAKKGSALEEPKATRL
Rat nNOS           1389RYHEDIFGVTLATYEVTNRLRSESIAFIEESKKDADEVFSS
Bovine eNOS        1155RYHEDIFGLTLRTQEVTSRIRTQSFSLQERHLRGAVPWAFDPPGPDTPGP
```

Fig. 1. Location of F1395 in nNOS. (*Upper*) Stacking interaction between phenyl of F1395 (green) and FAD isoalloxazine ring (blue) in a crystallized FNR fragment of nNOS (12). *Left* and *Right* of *Upper* are zoom out and 300% zooming picture of the FNR module of nNOS, respectively. (*Lower*) C-terminal sequence alignments for rat neuronal NOS (nNOS, SWISS-PROT accession no. P29476), mouse inducible NOS (iNOS, accession no. P29477), bovine endothelial NOS (eNOS, accession no. P29473), rat cytochrome P450 reductase (CYPR, accession no. P00388), spinach ferredoxin:NADP$^+$ reductase (FNR, accession no. P00455), *Escherichia coli*. sulfite reductase flavoprotein α-component (SIR-FP, accession no. P38038), and *Caenorhabditis elegans* methionine synthase reductase (MSR, accession no. Q17574). The conserved aromatic residue is marked by red.

primers as follows: F1395Y forward primer: AACGGTACCAC-GAGGACATC**TAT**GGAGTCACCCTCAGAACG. F1395Y reverse primer: AAATCTAGAAGGACCAGGACACAGC-AACAGGACAAG. F1395S forward primer: AACGGTACCA-CGAGGACATC**TCT**GGAGTCACCCTCAGAACG. F1395S reverse primer: AAATCTAGAAGGACCAGGACACAGCAA-CAGGACAAG. The restriction site and mutation site are denoted by underline and bold, respectively. The PCR product and wild-type pCWori vector containing nNOS DNA were digested by both the *Kpn*I and *Xba*I restriction enzymes. The double-digested fragment of the wild-type NOS-pCWori plasmid was replaced by the double-digested PCR fragment and transformed into JM109 cells to generate the recombinant plasmid. The sequence of mutation was confirmed by DNA sequencing at the Cleveland Clinic sequencing facility. F1395Y and F1395S in the pCWori plasmid were transformed into *Escherichia coli* strain BL21(DE3) for protein expression.

Expression and Purification of Wild-Type and Mutant Proteins. Wild-type rat nNOS and both mutant proteins had a His_6 tag attached to their N termini to aid purification. They were overexpressed in *E. coli* strain BL21(DE3) and purified by sequential chromatography on Ni^{2+}-NTA and 2′,5′-ADP-Sepharose as described (34).

Determination of Bound FAD and FMN. FAD and FMN were released from nNOS or mutants by heating at 95°C for 5 min in the dark and measured by using a fluorometric HPLC method as described (34).

NO Synthesis, NADPH Oxidation, Cytochrome *c* Reduction, and Ferricyanide Reduction. Steady-state activities of wild type and mutant proteins were determined separately at 25°C by using spectrophotometric assays that were described in detail (34).

Measurement of Apparent K_m for NADPH or NADH. Apparent K_m and V_{max} values were determined by double-reciprocal analysis of the NADPH-dependent cytochrome *c* reduction against various concentrations of NADPH or NADH in the presence of Ca^{2+}/CaM.

Heme and Flavin Reduction. Kinetics of flavins and heme reduction were analyzed at 10°C as described (32–34) by using a diode array

Table 1. Effect of F1395 mutations on steady-state nNOS activities

	Ferricyanide reduction, min^{-1}		Cytochrome *c* reduction, min^{-1}		NO synthesis, min^{-1}		NADPH oxidation, min^{-1}	
Enzyme	−CaM	+CaM	−CaM	+CaM	−CaM	+CaM	−CaM	+CaM
nNOS	1,000 ± 50	5,052 ± 500	500 ± 25	7,000 ± 400	0	55 ± 2	5.6 ± 1	110 ± 10
F1395Y	1,250 ± 30	6,059 ± 500	412 ± 18	6,090 ± 250	0	52 ± 2	5.2 ± 1	105 ± 8
F1395S	6,150 ± 500	5,550 ± 440	2,012 ± 200	2,025 ± 200	0.1	5.4 ± 0.8	48 ± 4	52 ± 5

BIOCHEMISTRY

Table 2. Effect of F1395 mutations on nicotinamide coenzyme utilization by nNOS

	NADPH		NADH	
Enzyme	Ferricyanide reduction, min^{-1}	Cytochrome *c* reduction, min^{-1}	Ferricyanide reduction, min^{-1}	Cytochrome *c* reduction, min^{-1}
nNOS	5,052 ± 500	7,000 ± 400	92 ± 3	60 ± 3
F1395Y	6,059 ± 500	6,090 ± 250	110 ± 5	56 ± 2
F1395S	5,550 ± 440	2,025 ± 200	2,851 ± 200	1,348 ± 40

detector and stopped-flow apparatus from Hi-Tech (Salisbury, U.K.; model SF-61) equipped for anaerobic work. Heme reduction was followed by formation of the ferrous-CO complex and the kinetics were determined by absorbance change at 444 nm. Reactions were initiated by rapidly mixing an anaerobic CO-saturated solution containing 100 μM NADPH with an anaerobic CO-saturated solution containing wild-type or mutant nNOS (2 μM), 40 mM 4-(2-hydroxyethyl)-1-piperazinepropanesulfonic acid (EPPS) buffer (pH 7.6), 10 μM 6*R*-tetrahydrobiopterin, 0.3 mM DTT, 1 mM Arg, 4 μM CaM, and 1 mM Ca^{2+}. Flavin reduction was monitored under the same conditions at 485 nm. Signal-to-noise ratios were improved by averaging at least 10 individual mixing experiments. The time course of absorbance change was fit to single- or multiple-exponential equations by using a nonlinear least-squares method provided by the instrument manufacturer.

Stability of Reduced Flavins. The reoxidation of reduced flavins was monitored for wild-type or mutant nNOS at 485 nm. nNOS proteins were diluted to 1.5 μM in air-saturated 40 mM EPPS buffer, pH 7.6, containing 0.9 mM EDTA, and reactions were started by adding 60 μM NADPH at room temperature.

Results

Characteristics of the F1395 Mutants. Spectroscopic analysis showed that the mutations did not affect the properties of the heme-containing oxygenase domain. Both mutants contained one FMN and one FAD per subunit (data not shown), which are normal quantities. As reported for wild type-nNOS (35), the F1395Y mutant contained an air-stable flavin semiquinone as judged by its having a broad absorbance centered at 590 nm. In contrast, F1395S nNOS contained fully oxidized flavins (data not shown).

Ferricyanide Reduction, Cytochrome *c* Reduction, and NO Synthesis. Table 1 compares various catalytic activities of wild-type and mutant nNOS enzymes. Ferricyanide and cytochrome *c* reductase activities in CaM-free F1395Y nNOS were similar to wild type and were increased to a normal extent on CaM binding. In contrast, CaM-free F1395S nNOS had markedly greater ferricyanide and cytochrome *c* reductase activities compared with wild type. The ferricyanide reductase activity of CaM-free F1395S was practically equivalent to that of CaM-bound nNOS, whereas its cytochrome *c* reductase activity was about 30% of that of CaM-bound nNOS. Binding CaM to F1395S nNOS did not further increase its ferricyanide or cytochrome *c* reductase activities.

CaM was obligatory for NO synthesis by F1395Y nNOS and supported a rate equivalent to wild-type enzyme. Corresponding NADPH oxidation rates for F1395Y nNOS in the absence or presence of CaM were similar to wild type, and indicated that NADPH oxidation by this mutant was well coupled to its NO synthesis. In contrast, CaM-free F1395S nNOS had a slow but detectable NO synthesis activity (equivalent to 0.2% of CaM-bound wild-type activity). Its NADPH oxidation rate was 8 times that of CaM-free wild type. CaM binding increased the NO synthesis activity of F1395S nNOS but only to 10% of that of wild type. Its NADPH oxidation under this condition was high and was mostly uncoupled from NO synthesis (Table 1).

Together, our steady-state catalytic measurements indicate that the aromatic side chain of F1395 is required to repress all three catalytic activities of nNOS in the absence of CaM. It also is needed to fully relieve repression of cytochrome *c* reduction and NO synthesis when CaM binds. The aromatic side chain of F1395 also prevents nNOS from catalyzing uncoupled electron transfer from NADPH to O_2 in the absence and presence of CaM.

Cofactor Affinity and Specificity. In view of the F1395 mutations causing probable alterations in nNOS-NADPH binding affinity and specificity (30, 31), we compared NADH vs. NADPH (0.3 mM each) as an electron donor for supporting ferricyanide and cytochrome *c* reductase activities (Table 2). Wild-type nNOS and the F1395Y mutant exhibited relatively low NADH-dependent ferricyanide and cytochrome *c* reductase activities. However, the F1395S mutant exhibited 33- and 23-fold faster ferricyanide and cytochrome *c* reduction at the same NADH concentration. These results suggest that Phe-1395 has a role in determining nicotinamide coenzyme specificity for nNOS.

We further investigated how the F1395 mutations affected utilization of NADPH or NADH. Table 3 summarizes apparent K_m and V_{max} values for NADPH and NADH determined by the cytochrome *c* reduction assay for CaM-bound wild-type and mutant nNOS proteins. For wild-type and the F1395Y mutant the apparent V_{max} was at least 4 times greater for reactions using NADPH than for those using NADH. However, for the F1395S mutant, the order was reversed such that the apparent V_{max} was highest for reactions using NADH. Comparing apparent K_m values indicated that wild-type and F1395Y nNOS exhibited a 1000-fold difference for NADPH vs. NADH, whereas F1395S nNOS showed only a 125-fold difference. Importantly, the

Table 3. Kinetic comparison of cytochrome *c* reductase activity supported by NADPH or NADH

	NADPH			NADH			NADPH/NADH
Enzyme	K_m, μM	V_{max}, min^{-1}	V_{max}/K_m (A), $\mu M^{-1}\cdot min^{-1}$	K_m, μM	V_{max}, min^{-1}	V_{max}/K_m (B), $\mu M^{-1}\cdot min^{-1}$	(A/B)
nNOS	4.8 ± 0.2	7,952 ± 700	1,656	5,000 ± 500	1,600 ± 100	0.32	4,987
F1395Y	4.0 ± 0.2	6,740 ± 650	1,685	4,400 ± 600	1,660 ± 50	0.377	4,469
F1395S	1.9 ± 0.1	2,726 ± 300	1,434	250 ± 15	3,464 ± 150	13.86	103

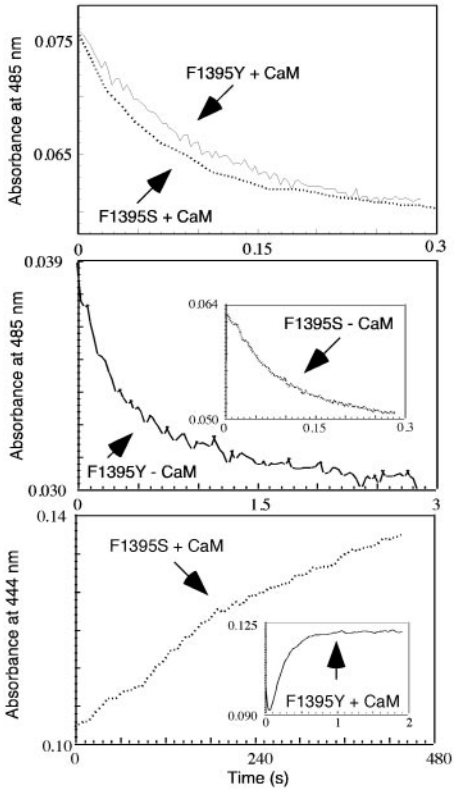

Fig. 2. Kinetics of NADPH-dependent flavin and heme reduction in F1395Y and F1395S. Flavin reduction was followed at 485 nm under anaerobic conditions at 10°C after mixing excess NADPH with CaM-bound (*Top*) or CaM-free (*Middle*) F1395Y and F1395S proteins. (*Bottom)* Heme reduction was detected by CO binding under anaerobic conditions and the kinetics were determined from the change in absorbance at 444 nm with time. CaM-bound enzymes were rapidly mixed with excess NADPH to trigger flavin and heme reduction at 10°C. Data shown are an average of 7–10 individual scans.

F1395S mutation resulted in a 20-fold increase in apparent K_m for NADH, but only a 2.2-fold increase in apparent K_m for NADPH. Comparison of V_{max}/K_m values indicated a 49-fold increased preference for NADH in F1395S nNOS compared with wild type. We conclude (*i*) the aromatic side chain of F1395 maintains nucleotide coenzyme specificity in nNOS mainly by discriminating against NADH, and (*ii*) the reduced specificity of F1395S nNOS is primarily because of changes in apparent K_m and V_{max} values for NADH.

Reduction of Flavins and Ferric Heme. To see whether F1395 controls electron transfer in nNOS, we compared rates of NADPH-dependent flavin and ferric heme reduction in the mutant and wild-type enzymes under anaerobic conditions. Reactions were initiated by mixing enzymes with a 33-fold excess of NADPH at 10°C. Flavin reduction was monitored at 485 nm, whereas heme reduction was followed by monitoring formation of the ferrous heme-CO complex at 444 nm (32–34).

Absorbance traces representing flavin reduction in CaM-free and CaM-bound nNOS proteins fit well to a biphasic process in all cases. As is shown in the *Top* and *Middle* of Fig. 2 and in Table 4, the kinetics of absorbance loss at 485 nm for CaM-bound F1395Y and F1395S mutants were similar to one another and also matched rates determined for CaM-bound wild-type nNOS. This result indicates that all three CaM-bound enzymes have generally similar flavin reduction kinetics. However, in the CaM-free state, we observed repressed rates of flavin reduction only in wild-type and F1395Y nNOS. Their fast phase rates were 10 and 5 times slower, respectively, compared with their CaM-bound forms. In contrast, flavin reduction in CaM-free F1395S nNOS was not significantly repressed, as judged by its having an observed rate of flavin reduction (fast phase) that was 70% the rate of the CaM-bound form. We conclude that the aromatic side chain of F1395 is needed to repress the rate of flavin reduction in CaM-free nNOS, but does not influence flavin reduction kinetics after CaM binds.

As shown in the *Bottom* and its *Inset* of Fig. 2, ferric heme reduction was much slower in F1395S than in the F1395Y mutant or in wild-type nNOS when they were compared in the CaM-bound state (Table 4). The F1395S mutation thus prevented heme reduction from achieving its normal speed on CaM binding. This effect likely explains why NO synthesis is slow in F1395S-nNOS (see Table 1).

NADPH Oxidation and Flavin Oxidation Kinetics. The facts that the F1395S mutant did not contain a flavin semiquinone after purification and had a high rate of NADPH oxidation in the absence of CaM suggest that the O_2 reactivity of its reduced flavin cofactors may be much greater when compared with wild-type nNOS. To test this hypothesis, we compared flavin reoxidation rates among CaM-free F1395S, F1395Y, and wild-type nNOS. The three enzymes at equal concentration were given the same amount of NADPH, and subsequent reduction and oxidation of their flavins was monitored over time at 485 nm. As shown in Fig. 3, the initial absorbance decrease after NADPH addition was almost twice as great for F1395S as compared with F1395Y or wild-type nNOS, consistent with only the latter two enzymes containing an air-stable FMN semiquinone at the start of the experiment. The F1395S flavins remained reduced for a shorter period compared with F1395Y and wild-type nNOS, as judged from the durations of their lag period before the final absorbance increase. This finding is consistent with the F1395S mutant consuming NADPH 8 times faster under this circumstance (see Table 1). The slopes of the absorbance increase once NADPH had become depleted indicated that flavin reoxidation was about 20 times faster in F1395S mutant than in wild-type or F1395Y enzymes. Their observed rates (ΔA at 485 nm) were estimated to be 1.98 min^{-1}, 0.08 min^{-1}, and 0.072 min^{-1}, respectively. The magnitude of absorbance changes during flavin reoxidation indicates that wild-type and F1395Y enzymes were

Table 4. Rates for flavin reduction and heme reduction in wild-type and mutant nNOS

	Flavin reduction, s^{-1}				
	+CaM		−CaM		
Enzyme	k_1	k_2	k_1	k_2	Heme reduction, s^{-1}
Wild type	23 ± 2 (54%)	3.4 ± 0.3 (46%)	2.3 ± 0.2 (18%)	0.9 ± 0.1 (82%)	3.9 ± 0.3
F1395Y	22 ± 2 (60%)	3.0 ± 0.2 (40%)	4.4 ± 1.3 (50%)	0.8 ± 0.1 (50%)	3.6 ± 0.4
F1395S	28 ± 2 (50%)	6.0 ± 0.5 (50%)	19 ± 2 (43%)	6.1 ± 0.5 (57%)	0.005 ± 0.001

k_1 and k_2 are rates for the fast and slow phases, respectively. Percentages of absorbance change for each phase are in parentheses.

BIOCHEMISTRY

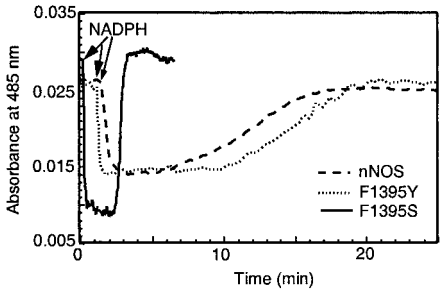

Fig. 3. Stability of reduced flavins. The reduction and reoxidation of reduced flavins was monitored for wild-type or mutant nNOS at 485 nm. nNOS proteins were diluted to 1.5 μM in air-saturated 40 mM EPPS buffer, pH 7.6, containing 0.9 mM EDTA, and reactions were started by adding 60 μM NADPH at room temperature.

left containing a stable FMN semiquinone, whereas the F1395S mutant was left containing fully oxidized flavins.

Discussion

F1395S nNOS had an increased affinity toward NADPH and NADH, but a reduced ability to discriminate between them. These characteristics suggest that F1395 influences NADPH/NADH binding according to principles outlined for analogous aromatic residues in related flavoproteins (30, 31, 36). Essentially, the phenyl side chain of F1395 may antagonize productive stacking between bound FAD cofactor and the reduced nicotinamide ring of NADPH or NADH, and may also help dissociate oxidized nicotinamide coenzyme from the nNOS binding site after hydride transfer to FAD occurs. In these ways the F1395S mutation could increase nNOS binding affinity toward both NADPH and NADH. However, the mutational effects may be more pronounced on NADH binding because that process does not involve protein interactions with the 2′-phosphate, and consequently relies more on protein–nicotinamide interactions (36).

CYPR and FNR mutants that are missing the corresponding aromatic side chain exhibit a 80- to 150-fold increase in their NADPH/$NADP^+$ affinity (30, 36). In contrast, the NADPH affinity of F1395S nNOS was increased only slightly over wild type as indicated by a 2-fold difference in apparent K_m for NADPH (Table 3). The small mutational effect is consistent with NADPH binding being more reliant on protein interactions with the 2′-phosphate group. It is also catalytically significant because it appears to keep $NADP^+$ release from becoming rate limiting for electron transfer reactions catalyzed by F1395S nNOS, as otherwise occurs in analogous CYPR and FNR mutants that are missing the aromatic side chain (30, 31, 36). This concept is demonstrated by CaM-free F1395S nNOS having increased ferricyanide or cytochrome *c* reductase activities compared with CaM-free wild-type nNOS (Table 1). The increased activities of F1395S nNOS could not have occurred if $NADP^+$ release became rate limiting. Thus, the aromatic side chain of F1395 may not be essential for timely displacement of $NADP^+$ from nNOS, and therefore is likely to impact catalysis by a different mechanism.

We also found that the aromatic side chain of F1395 is needed to stabilize the FMN semiquinone and, perhaps, hydroquinone states against air oxidation. Because the C-terminal control element of nNOS also protects its reduced flavins from air oxidation (21–23), F1395 may function through an effect on the C-terminal element. However, this is not necessarily the case, because destabilization of the FMN semiquinone also occurs in similar CYPR mutants (30), despite their not having a C-terminal control element. In any case, it will be important to understand the structural basis for the protection because it keeps NADPH oxidation coupled to NO synthesis and minimizes nNOS production of reduced oxygen species such as H_2O_2 or superoxide.

Remarkably, we found that the phenyl side chain of F1395 governs electron transfer both into and out of the nNOS reductase domain. This role is unexpected and stands to broaden our understanding of flavoproteins. Evidence that F1395 regulates electron flux in CaM-free nNOS includes the following: (*i*) the F1395S mutant displayed faster flavin reduction and greater ferricyanide and cytochrome *c* reductase activities as compared with wild-type nNOS; and (*ii*) F1395 nNOS displayed some NO synthesis and, therefore, heme reduction, which does not occur in CaM-free nNOS. These effects contrast from what is seen for comparable aromatic residues in CYPR and FNR. In these enzymes, removal of the aromatic side chain causes little change in their flavin reduction rates. It also slows down their ferricyanide or cytochrome *c* reductase activities and cytochrome P450-dependent reactions because of a slower $NADP^+$ release (30, 31). Thus, besides having a prototypical role in controlling NADPH/NADH binding specificity, F1395 has an additional unique function in regulating nNOS electron transfer.

CaM binding relieves repression of electron transfer into and out of the nNOS reductase domain (14, 18). Because the F1395S mutation relieved some of the repression in CaM-free nNOS, we conclude that the aromatic side chain of F1395 must help to repress electron transfer. It also appears essential for proper response to CaM. This concept is demonstrated by CaM-bound F1395S nNOS having slower cytochrome *c* reductase activity, heme reduction, and NO synthesis, compared with CaM-bound wild-type nNOS. Thus, the aromatic side chain of F1395 is needed to repress electron transfer and to fully relieve the repression once CaM binds. Remarkably, the same holds true for the autoinhibitory insert and C-terminal control elements as shown through deletion studies (19–22). In particular, the catalytic profile of a C-terminal-deleted nNOS (21) is quite similar to that of our F1395S mutant. We speculate that proper negative and positive functions of the C-terminal control element require and possibly involve the F1395 aromatic side chain. The following conceptual model is consistent with results to date. In the CaM-free state, the autoinhibitory insert and C-terminal control elements act in conjunction with F1395 to repress electron transfer into and out of the nNOS reductase domain. When CaM binds, the repression by these elements is relieved and F1395 functions primarily like analogous aromatic residues in related flavoproteins to control NADPH-binding specificity. Removal of the F1395 aromatic side chain prevents proper repressive functioning of the C-terminal element, and also diminishes its ability to relieve repression once CaM is bound.

How might F1395 regulate electron transfer events in conjunction with the C-terminal element? Its influence on the C-terminal element is easy to imagine because F1395 lies immediately upstream in sequence (see Fig. 1). Perhaps it is simplest to consider how F1395 might repress electron import into the reductase domain of CaM-free nNOS. A crystal structure of an nNOS FNR fragment shows that the phenyl ring of F1395 stacks nearly parallel with the isoalloxazine ring of FAD, and thus can block stacking between FAD and reduced nicotinamide as required for hydride transfer (12). One mechanism would have the C-terminal element stabilize the F1395 phenyl–FAD stacking interaction such that forming a productive nicotinamide–FAD stacking interaction (which requires the phenyl group to swing away) becomes rate limiting. Alternatively, the phenyl side chain of F1395 might act in conjunction with the C-terminal control element to stabilize a nonoptimal stacking geometry between FAD and nicotinamide in CaM-free nNOS. Binding CaM would then alter the C-terminal control element such that the negative effects were removed.

Cytochrome *c* reduction, NOS heme reduction, and NO synthesis were also altered in F1395S nNOS. Besides involving

hydride transfer between NADPH and FAD, these activities require electrons to pass from FAD to FMN and then out from the reductase domain to an exogenous hemeprotein or the NOS heme. Their inherent complexity makes interpretation difficult, but we know that F1395 has both positive and negative effects on these downstream electron transfer events, depending on whether CaM is bound or not. Recently, Daff and colleagues (37) reported that NADPH or $NADP^+$ must be bound for these activities to be repressed in CaM-free nNOS. Their finding provides a clue to F1395 function. Because the phenyl side chain of F1395 can flip away from FAD to accommodate NADPH or $NADP^+$, we suspect that phenyl side chain movement is a component of a conformational trigger mechanism that regulates electron transfer out of the nNOS reductase domain. This side chain movement would act in conjunction with and influence the C-terminal and autoinhibitory control elements. In this model, binding NADPH or $NADP^+$ to nNOS causes phenyl side chain displacement that triggers repression of electron export from CaM-free nNOS. The same movement may trigger full relief of repression once CaM is bound. Such use of the conserved aromatic residue would be in keeping with other unique aspects of the nNOS flavoprotein (19–26) and certainly deserves further investigation.

In summary, our work identifies NOS as, to our knowledge, the first redox protein to use the conserved aromatic shielding residue to control electron transfer into and out of its flavoprotein. This finding helps to explain how CaM can regulate a redox enzyme such as NOS. These concepts together provide a different structure–function perspective on flavoproteins, particularly in how residues surrounding the NADPH–FAD interface can participate in more global and distant regulatory processes, and thus be used in ways much broader than previously imagined.

We thank Elsa Garcin and Dr. Elizabeth Getzoff of the Scripps Research Institute for helpful discussions. This work was supported by National Institutes of Health Grant GM51491 (to D.J.S.) and a grant from the American Heart Association (to S.A.).

1. Ignarro, L. J., ed. (2000) *Nitric Oxide, Biology and Pathobiology* (Academic, San Diego).
2. Furchgott, R. F. (1999) *Biosci. Rep.* **19,** 235–251.
3. Stuehr, D., Pou, S. & Rosen, G. M. (2001) *J. Biol. Chem.* **276,** 14533–14536.
4. Pferiffer, S., Mayer, B. & Hemmens, B. (1999) *Angew. Chem. Int. Ed. Engl.* **38,** 1714–1731.
5. Roman, L. J., Martasek, P. & Masters, B. S. (2002) *Chem. Rev.* **102,** 1179–1190.
6. Crane, B. R., Arvai, A. S., Ghosh, D. K., Wu, C., Getzoff, E. D., Stuehr, D. J. & Tainer, J. A. (1998) *Science* **279,** 2121–2126.
7. Raman, C. S., Li, H., Martasek, P., Kral, V., Masters, B. S. & Poulos, T. L. (1998) *Cell* **95,** 939–950.
8. Fischmann, T. O., Hruza, A., Niu, X. D., Fossetta, J. D., Lunn, C. A., Dolphin, E., Prongay, A. J., Reichert, P., Lundell, D. J., Narula, S. K. & Weber, P. C. (1999) *Nat. Struct. Biol.* **6,** 233–242.
9. Wang, M., Roberts, D. L., Paschke, R., Shea, T. M., Masters, B. S. & Kim, J. J. (1997) *Proc. Natl. Acad. Sci. USA* **94,** 8411–8416.
10. Olteanu, H. & Banerjee, R. (2001) *J. Biol. Chem.* **276,** 35558–35563.
11. Gruez, A., Pignol, D., Zeghouf, M., Coves, J., Fontecave, M., Ferrer, J. L. & Fontecilla-Camps, J. C. (2000) *J. Mol. Biol.* **299,** 199–212.
12. Zhang, J., Martasek, P., Paschke, R., Shea, T., Masters, B. S. & Kim, J. J. (2001) *J. Biol. Chem.* **276,** 37506–37513.
13. Marletta, M. A., Hurshman, A. R. & Rusche, K. M. (1998) *Curr. Opin. Chem. Biol.* **2,** 656–663.
14. Abu-Soud, H. M. & Stuehr, D. J. (1993) *Proc. Natl. Acad. Sci. USA* **90,** 10769–10772.
15. Lambeth, J. D. (2002) *Curr. Opin. Hematol.* **9,** 11–17.
16. Agostinho, M., Oliveira, S., Broco, M., Liu, M. Y., LeGall, J. & Rodrigues-Pousada, C. (2000) *Biochem. Biophys. Res. Commun.* **272,** 653–656.
17. Matsuda, H. & Iyanagi, T. (1999) *Biochim. Biophys. Acta* **1473,** 345–355.
18. Abu-Soud, H. M, Yoho, L. L. & Stuehr, D. J. (1994) *J. Biol. Chem.* **269,** 32047–32050.
19. Salerno, J. C., Harris, D. E., Irizarry, K., Patel, B., Morales, A. J., Smith, S. M., Martasek, P., Roman, L. J., Masters, B. S., Jones, C. L., *et al.* (1997) *J. Biol. Chem.* **272,** 29769–29777.
20. Daff, S., Sagami, I. & Shimizu, T. (1999) *J. Biol. Chem.* **274,** 30589–30595.
21. Roman, L. J., Martasek, P., Miller, R. T., Harris, D. E., de La Garza, M. A., Shea, T. M., Kim, J. J. & Masters, B. S. (2000) *J. Biol. Chem.* **275,** 29225–29232.
22. Montgomery, H. J., Romanov, V. & Guillemette, J. G. (2000) *J. Biol. Chem.* **275,** 5052–5058.
23. Roman, L. J., Miller, R. T., de La Garza, M. A., Kim, J. J. & Masters, B. S. (2000) *J. Biol. Chem.* **275,** 21914–21919.
24. Nishida, C. R. & Ortiz de Montellano, P. R. (1999) *J. Biol. Chem.* **274,** 14692–14698.
25. Chen, P. F. & Wu, K. K. (2000) *J. Biol. Chem.* **275,** 13155–13163.
26. Lane, P. & Gross, S. S. (2002) *J. Biol. Chem.* **277,** 19087–19094.
27. Hubbard, P. A., Shen, A. L., Paschke, R., Kasper, C. B. & Kim, J. J. (2001) *J. Biol. Chem.* **276,** 29163–29170.
28. Serre, L., Vellieux, F. M., Medina, M., Gomez-Moreno, C., Fontecilla-Camps, J. C. & Frey, M. (1996) *J. Mol. Biol.* **263,** 20–39.
29. Pai, E. F., Karplus, P. A. & Schulz, G. E. (1988) *Biochemistry* **27,** 4465–4474.
30. Döhr, O., Paine, M. J., Friedberg, T., Roberts, G. C. & Wolf, C. R. (2001) *Proc. Natl. Acad. Sci. USA* **98,** 81–86.
31. Gutierrez, A., Döhr, O., Paine, M., Wolf, C. R., Scrutton, N. S. & Roberts, G. C. (2000) *Biochemistry* **39,** 15990–15999.
32. Adak, S., Aulak, K. S. & Stuehr, D. J. (2001) *J. Biol. Chem.* **276,** 23246–23252.
33. Adak, S., Santolini, J., Tikunova, S., Wang, Q., Johnson, J. D. & Stuehr, D. J. (2001) *J. Biol. Chem.* **276,** 1244–1252.
34. Adak, S., Ghosh, S., Abu-Soud, H. M. & Stuehr, D. J. (1999) *J. Biol. Chem.* **274,** 22313–22320.
35. Stuehr, D. J. & Ikeda-Saito, M. (1992) *J. Biol. Chem.* **267,** 20547–20550.
36. Piubelli, L., Aliverti, A., Arakaki, A. K., Carrillo, N., Ceccarelli, E. A., Karplus, P. A. & Zanetti, G. (2000) *J. Biol. Chem.* **275,** 10472–10476.
37. Craig, D. H., Chapman, S. K. & Daff, S. (2002) *J. Biol. Chem.* **277,** 33987–33994.